Biophysical Journal, Volume 98

Supporting Material

Gadolinium ions block mechanosensitive channels by altering the packing and lateral pressure of anionic lipids

Yuri Ermakov, Kishore Kamaraju, Krishnendu Sengupta, and Sergei I. Sukharev

Supplemental material to the paper

Gadolinium ions block mechanosensitive channels by altering the packing and lateral pressure of anionic lipids

by Yury A. Ermakov[1], Kishore Kamaraju[3] Krishnendu Sengupta[2] and Sergei Sukharev[3]

[1]*The Frumkin Institute of Physical Chemistry and Electrochemistry, Russian Academy of Sciences, Leninsky Prosp. 31, Moscow 119991, Russia*
[2]*Indian Association for the Cultivation of Sciences, 2A&2B Raja S C Mullick Road, Kolkata 700032, West Bengal, INDIA*
[3]*Department of Biology, University of Maryland, College Park, MD 20742*

MATERIALS AND METHODS

MscL reconstitution and recording in the presence of Gd^{3+}. MscL protein with a C-terminal 6His tag was expressed from the p5-2-2b vector in PB104 (ΔΩ3a) *E. coli* (*mscL*-) cells and purified on a Ni-NTA column (Qiagen) as described previously (Sukharev et al., 1999). Solubilization and purification was done in the presence of Octylglucoside (Calbiochem) (10 mg/ml) and soybean phosphatidylcholine (0.2 mg/ml). Two lipid compositions were used for protein reconstitution: one was soybean phosphatidylcholine (Sigma, type IV-S), a practically neutral mixture of natural phospholipids, and another was the same phosphatidylcholine with added porcine brain phosphatidylserine (Avanti) at a molar ratio of 7:3. The protein was reconstituted with lipids solubilized in octylglucoside at the ratio of 1:300 (wt/wt). The detergent was removed by 24-hr dialysis; the formed proteoliposomes were spun down and subjected to a dehydration-rehydration cycle as previously described (Sukharev et al., 1993). Large unilamellar blisters were induced by 10-20 min exposure of liposome aggregates to distilled water, which was then gradually replaced by the recording buffer (200 mM KCl, 40 mM $MgCl_2$, 10 mM Hepes-KOH, pH 7.2). Borosilicate pipettes of 2 MOhm were used to record MscL activities in excised patches. Activating pressure ramps were delivered from an HSPC-1 pressure clamp machine (ALA Scientific Instr.). $GdCl_3$ was delivered to the bath solution with a laboratory-built perfusion system.

Monolayer experiments. DMPS, DMPC, and in some experiments dimyrystoyl phosphatidylglycerol (DMPG) were from Avanti Polar Lipids (Alabaster, AL). $GdCl_3$, Tris, 2-(N-Morpholino) ethanesulfonic acid (MES) and EDTA, all of analytical grade, were purchased from Sigma-Aldrich (St. Louis, MO). Measurements were performed at a fixed ionic strength and pH 7.0 in the subphase (10 mM KCl, 2 mM *Tris*-HCl), unless stated otherwise. Subphase solutions were prepared with MilliQ water (18 MOhm·cm). Potassium chloride (Fluka, Buchs, Switzerland), used as the background electrolyte, was pre-heated to *ca*. 900 K to eliminate organic impurities. Monolayers were formed by spreading 0.5 mM solutions of phospholipids dissolved in freshly distilled chloroform. Measurements were begun upon complete evaporation of chloroform from the surface.

Surface pressure and interfacial potential isotherms were measured simultaneously in a Langmuir trough at room temperature (~23^{o} C) with a Wilhelmy balance and a surface (Volta) potential meter (Kelvin probe) as described previously (Shapovalov and Tronin, 1997). The measurements with 100% of DMPS in the presence of lanthanides revealed significant

hysteresis, thus the data from such experiments represent the compression phase only. Area compressibility moduli were calculated according to the equation $C_S = (-1/A)(dA/d\pi)$ (Smaby et al., 1997).

The principles of surface potential measurements on monolayers have been previously reviewed by Brockman (Brockman, 1994). The total surface potential measured with a Kelvin probe includes both the dipole component created by the layers of oriented molecules and the diffuse part of the electrical double layer (EDL) created by ionized groups and counterions in the aqueous subphase. The latter is usually approximated by the Gouy-Chapman-Stern (GCS) model (McLaughlin et al., 1981).

A three-electrode circuit was used in our laboratory-built surface potential meter. It included a polished gold-coated vibrating electrode (1 cm in diameter) with the vibration frequency of 70 Hz and 0.2 mm amplitude. The plate was lowered to the distance of about 1 mm above the surface upon complete evaporation of the solvent (chloroform). For the purpose of stability, an auxiliary (grounding) electrode made of stainless steel was placed in the water phase under the vibrating plate in addition to an Ag/AgCl reference electrode. As a result, the accuracy and long-term stability were 5 and 10 mV, respectively. All surface potential curves were reproducible within 10 mV in the range of surface pressures above 0.5 mN/m.

Isothermal titration experiments. The assays for ion binding affinity were performed with DMPS liposomes prepared by extrusion of a pre-heated suspension through a 100 nm Nucleopore filter. The buffer contained 10 mM KCl and 5 mM Hepes (pH 7.2). Measurements were conducted on a Microcal VP-ITC calorimeter. In a typical experiment, 2-5 μl injections of 1 mM Gd^{3+} solution were delivered into the cell containing 1.45 ml of 0.3 mM DMPS suspension. Prior to injections, the cells were equilibrated at either 25 or 45^{o}C to perform measurements on lipids below or above phase transition, which occurs between 39 and 41^{o}C for DMPS in KCl electrolytes (Marsh, 1990). The heat responses were integrated and analyzed with the MicroCal Origin (version 7) software. The MicroCal LLC routine was used to analyze ITC data. The experimental curves were fitted by one-site or two-site binding models.

The 'benchmark' experiments on Langmuir monolayers presented below provided us the scale of effects caused by simple neutralization of DMPS charges with acid, by interacting with a 1:1 monovalent electrolyte or by mixing with neutral DMPC.

Fig. S1A depicts a series of pressure-area (π-A) isotherms obtained at different pH values. At neutral and basic pH (7-9), the compression isotherms coincide and show the steepest pressure increase with compression and a LE-LC transition at around 25 mN/m signifying high electrostatic repulsion and a maximally charged state of the molecules in the film. A decrease of pH from 7 to 3 delays the pressure onset upon compression and sharply decreases the phase transition pressure to ~7 mN/m. The positions of the surface potential curves (Fig. S1B) reflecting both the dipole and the electric double layer (EDL) components are consistent with progressive neutralization. The total down-shift of surface potential with a pH change from 2 to 7 is approximately 100 mV, which roughly corresponds to the diffuse part of the surface potential estimated at the given density of charges in the GCS approximation. The increased headgroup ionization progressively made the surface potential more negative in both liquid-expanded and condensed states. Consistent with the previous electrokinetic measurements (Ermakov et al., 1997), at pH 2 the surface charge of PS should be close to zero (Tocanne and Teissie, 1990), and thus in the monolayer it may not contribute to the total surface potential. The measured surface potential in this case has only the dipole component, which increases as the lipid packing becomes tighter.

The long-range electrostatic repulsion at high pH apparently extends the range of π-A diagrams to the right, but at low pH, the lateral pressure is detectable only at areas around 0.75 nm^2 per molecule (Fig. S1A). Most 'neutral' monolayers at pH 2 produced a sharp onset of the dipole potential (~300 mV) preceding the detectable raise of surface pressure (Fig. S1B), previously described by Brockman (Smaby and Brockman, 1990; Brockman, 1994). We did not attempt to interpret the observed difference in steepness of the dipole potential's onset between the fully charged and partially neutralized films (Fig. S1B). It has been shown recently that the surface potential isotherms in the region of 2D-gas – LE phase coexistence at which lateral pressure is still undetectable are strongly influenced by thermally induced macroscopic streams at the surface. These conditions are difficult to control, and thus the expanded region of surface potential isotherms is usually poorly reproducible in contrast to the remaining part (Shapovalov et al., 2002).

The second 'benchmark' experiment presented in Fig. S2 illustrates the effect of charge density variation achieved through different PS/PC content in the lipid mixture. The compression isotherm for pure DMPC shows no visible break of its slope, signifying the absence of phase transition (Ali et al., 1998); the transition, however is vividly present in pure DMPS. The mixtures display intermediate behavior, and a phase transition is seen only when DMPS constitutes 50% or more. Importantly, before the onset of phase transition, the compression isotherms for DMPC and DMPS essentially coincide, indicating that the headgroup specificity starts playing its role in packing at the molecular areas below 0.6 nm^2. Higher compressibility of DMPS is apparently conferred by its smaller headgroup capable of hydrogen bonding (Cevc et al., 1981; Leberle et al., 1989; Slater et al., 1993; Mukhopadhyay et al., 2004). The slopes of surface potential curves also change with the onset of the phase transition, which is pronounced again only at high DMPS/DMPC ratios. We should note that in our previous study, the dipole

potential at the surface of the planar lipid membrane became sensitive to the presence of polyvalent ions also when the fraction of charged PS was higher than 50% (Ermakov et al., 2001). Correspondingly, the spacing between interfacial potential traces is not the same at different packing densities.

In the third 'benchmark' experiment illustrated in Fig. S1 we varied the concentration of KCl in the subphase to see the effects of the surface charge screening by a 1:1 electrolyte. Previously, it has been shown for a number of charged lipids and surfactants that the varying concentration of the background electrolyte defines the surface potential in the double layer, but does not change the shape of compression isotherms (Shapovalov and Brezesinski, 2006). This somehow counters the expectation that increased ionic strength should reduce repulsion, making the film effectively 'softer' and possibly lowering the surface pressure for the LE-LC phase transition. In this experiment, we chose KCl to be the major background electrolyte, thus the measurements were done in the presence of 0.4-4 mM EDTA (see legend to Fig. S2) which served as a buffer and removed multivalent impurities. Fig. S3A shows that the lowest concentrations of electrolyte (10^{-3} M) produced more easily compressible films with lower transition pressures as if the lipid charges were effectively neutralized (see Fig.3, main text), whereas higher KCl concentrations produced control-like curves. The critical pressures for the LE-LC transitions were 13, 21 and 23 mN/m at 1, 10 and 100 mM, respectively. The positions of surface potential curves were consistent with the gradual decrease of the diffuse component of the surface potential, producing incremental upward shifts of about 50 mV per tenfold increase of salt concentration, suggesting that the charge density remains roughly the same and KCl indeed behaves almost like an indifferent electrolyte (Shapovalov and Brezesinski, 2006). Since these measurements were performed at pH 6, not all PS headgroups are expected to be ionized. With increased ionic strength (KCl), we may expect lowering the potential in the double layer and additional deprotonation of PS, which in turn increases the surface charge density. The competition between K^+ and H^+ binding to PS has been considered previously (McLaughlin, 1989; Ermakov et al., 2001) and increase of K^+ concentration is expected to liberate protons from the surface increasing the charge density. The higher charge in turn may make the monolayer stiffer, as illustrated in Fig. S3. Under conditions of complete ionization of PS headgroups (at pH 9-10), compression isotherms do not change their shape with ionic strength (data not shown).

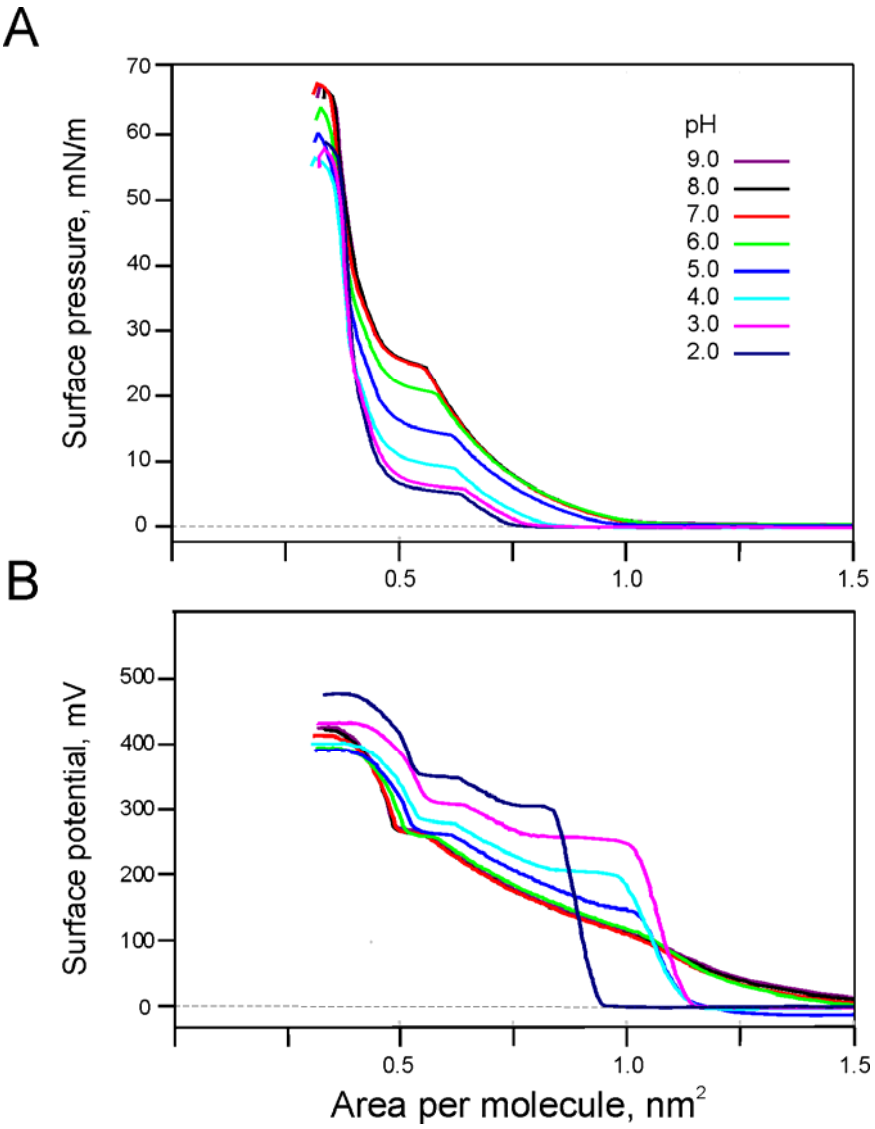

Fig. S1. Pressure-area (A) and surface potential-area (B) diagrams for monolayers formed form DMPS taken at different pH. The subphase electrolyte contained 10 mM KCl, 0.3 mM EDTA; pH was adjusted by adding appropriately diluted KOH or HCl.

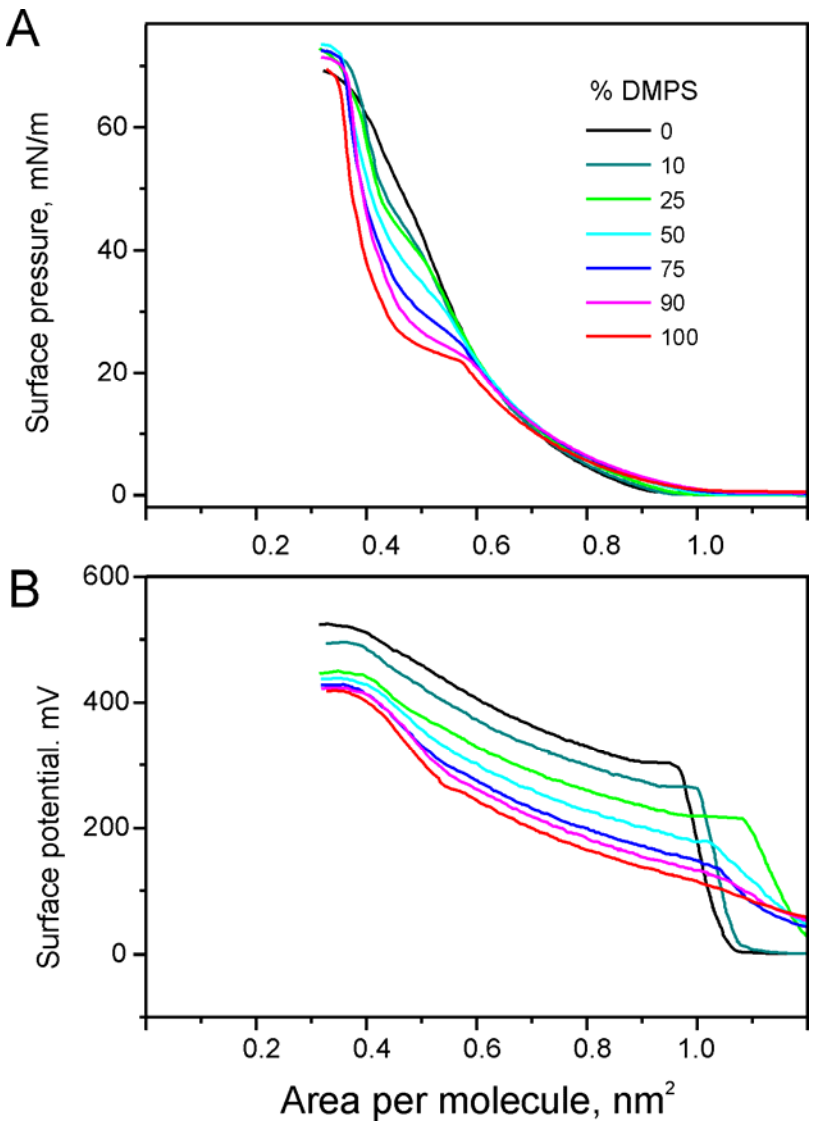

Fig. S2. Pressure-area (A) and surface potential-area (B) diagrams for monolayers formed from mixtures of DMPS and DMPC (see color coding in A).

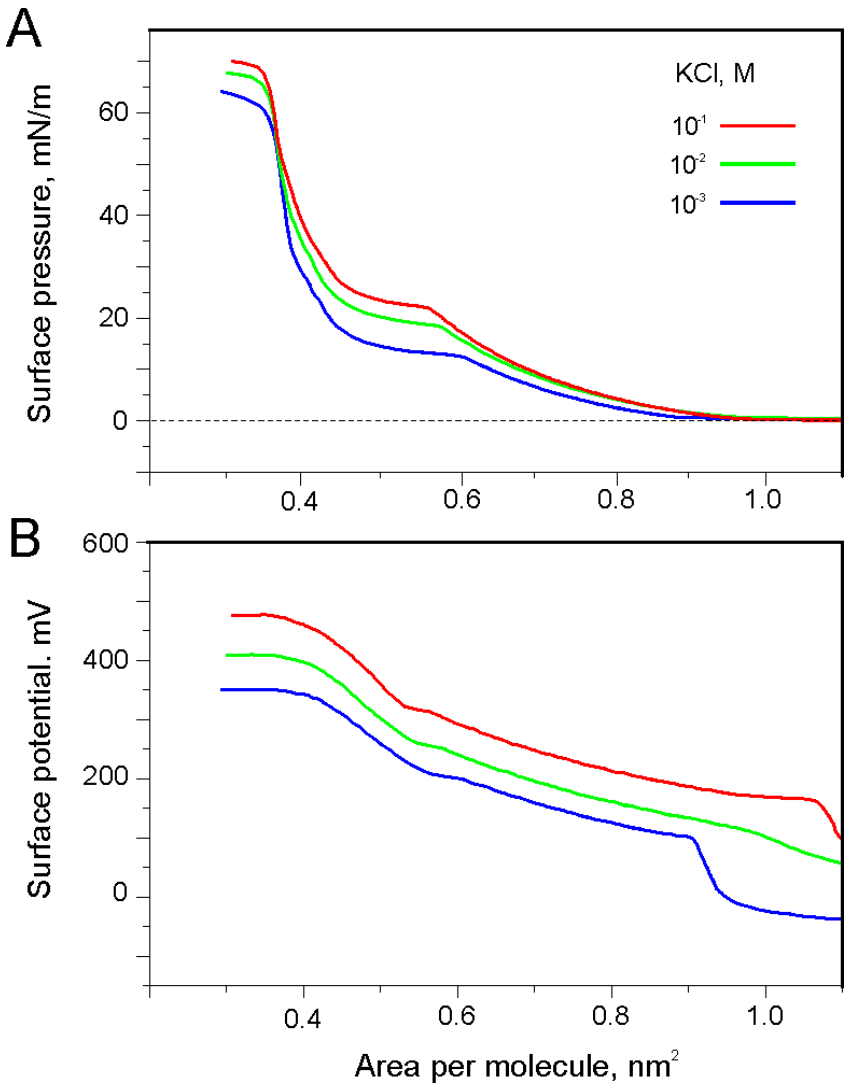

Fig. S3. Pressure-area (A) and surface potential-area (B) diagrams for DMPS monolayers spread over subphases containing different concentrations of the background electrolyte KCl (see color coding in A). All measurements were carried out in the presence of K_2EDTA as a buffer adjusted to pH 6.0. The exact buffer compositions for each experiment: 0.4 mM K_2EDTA+0.2 mM KOH; 4 mM K_2EDTA+2 mM KOH; 90 mM KCl+ 4 mM K_2EDTA+2 mM KOH.

Derivation of equation for compressive pressure acting on a membrane protein

In this section, we present a derivation of the pressure *p* exerted on a cylindrical protein of radius *r* inserted in the center of a discoid lipid domain of radius *R* undergoing condensation as shown schematically in Fig. S4. For simplicity, we first assume that the pressure *p* at the inner rim *r* is such that the expansion of the protein leads to a change in the radius of the inner rim by αr, where α is the relative linear contraction.

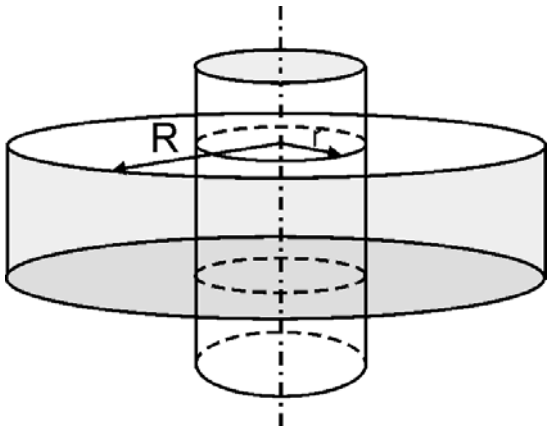

Fig. S4. A cartoon representing a cylindrical protein surrounded by a circular cluster of charged lipids receptive to modification by Gd^{3+}. R and r represent the radii of the lipid ring and the protein, correspondingly. Ion binding changes the area per lipid, correspondingly reducing the linear dimensions of the lipid ring. The 'shrinkage' exerts lateral pressure on the protein.

The pressure at the edge of the lipid domain at radius R is assumed to be zero. In general, at any radial distance *x* between the radii *r* and *R*, one may define a displacement field *u(x)* which obeys (Landau and Lifshitz, 1987)

$$\nabla^2 u(x) = 0 \qquad (1)$$

and satisfies the boundary condition $u(r)=\alpha r$. Due to the radial symmetry of the problem, as evident from Fig. 6, one can write the solution of Eq. (1) as

$$u(x) = Ax + \frac{B}{x} \qquad (2)$$

The boundary condition at the inner radius *r* leads to the equation

$$A + \frac{B}{r^2} = \alpha \qquad (3)$$

The strain caused by the this displacement can be computed from the strain tensor

whose radial and angular components are given by

$$e_{xx} = A - \frac{B}{x^2} \qquad e_{\varphi\varphi} = A + \frac{B}{x^2} \tag{4}$$

where φ is the azimuthal angle. This strain tensor is related to the stress tensor through the Poisson's ratio σ and the Young's modulus *E*

$$s_{ij} = \frac{E}{1+\sigma}\left(e_{ij} + \frac{\sigma}{1-2\sigma}\delta_{ij}\sum_l e_{ll} \right) \tag{5}$$

The radial and angular components of the stress tensor are given by

$$s_{xx} = \beta\left(A - \frac{B}{x^2}(1-2\sigma) \right) \qquad s_{\varphi\varphi} = \beta\left(A + \frac{B}{x^2}(1-2\sigma) \right) \tag{6}$$

where $\beta = E/[(1+\sigma)(1-2\sigma)]$. Since the pressure at a radial distance *x* is related to the stress tensor s_{xx} by $s_{xx} = -p_x(x)$, we find the boundary condition that the pressure vanish at the outer rim leads to the equation

$$A - \frac{B}{R^2}(1-2\sigma) = 0 \tag{7}$$

Using Eqs. 3 and 7, we find the coefficients *A* and *B* to be

$$A = C(1-2\sigma) \qquad B = CR^2 \qquad C = r^2\alpha \Big/ [r^2(1-2\sigma) + R^2] \tag{8}$$

Substituting Eq. 8 in Eq. 6, we find that the radial component of the stress tensor to be

$$s_{xx} = \frac{EC}{1+\sigma}\left(1 - \frac{R^2}{x^2} \right) \tag{9}$$

which leads to the final expression for the pressure *p* at the inner rim radius *r*

$$p = -s_{xx}(x=r) = \frac{E\alpha\left(1 - r^2/R^2\right)}{(1+\sigma)\left[1 + (1-2\sigma)r^2/R^2\right]} \tag{10}$$

Reference List

1. Ali, S., J. M. Smaby, M. M. Momsen, H. L. Brockman, and R. E. Brown. 1998. Acyl chain-length asymmetry alters the interfacial elastic interactions of phosphatidylcholines. *Biophys J* 74:338-348.

2. Brockman, H. 1994. Dipole Potential of Lipid-Membranes. *Chemistry and Physics of Lipids* 73:57-79.

3. Cevc, G., A. Watts, and D. Marsh. 1981. Titration of the phase transition of phosphatidylserine bilayer membranes. Effects of pH, surface electrostatics, ion binding, and head-group hydration. *Biochemistry* 20:4955-4965.

4. Ermakov, Y. A., A. Z. Averbakh, A. I. Yusipovich, and S. Sukharev. 2001. Dipole potentials indicate restructuring of the membrane interface induced by gadolinium and beryllium ions. *Biophys J* 80:1851-1862.

5. Ermakov, Y., A. Z. Averbakh, and S. I. Sukharev. 1997. Lipid and cell membranes in the presence of gadolinium and other ions with high affinity to lipids. 1. Dipole and diffuse components of the boundary potential. *Membr Cell Biol* 11:539-554.

6. Landau, L. D. and E. M. Lifshitz. 1987. Fluid Mechanics. Course of Theoretical Physics, Volume 6. Butterworth-Heinemann, New York.

7. Leberle, K., I. Kempf, and G. Zundel. 1989. An Intramolecular Hydrogen-Bond with Large Proton Polarizability Within the Head Group of Phosphatidylserine - An Infrared Investigation. *Biophysical Journal* 55:637-648.

8. Mukhopadhyay, P., L. Monticelli, and D. P. Tieleman. 2004. Molecular dynamics simulation of a palmitoyl-oleoyl phosphatidylserine bilayer with Na+ counterions and NaCl. *Biophysical Journal* 86:1601-1609.

9. Shapovalov, V. L., B. R. Shub, and O. N. Oliveira. 2002. Thermal Marangoni flows and macroscopic domain movement in monolayer surface potential experiments. *Colloids and Surfaces A-Physicochemical and Engineering Aspects* 198:195-206.

10. Slater, S. J., C. Ho, F. J. Taddeo, M. B. Kelly, and C. D. Stubbs. 1993. Contribution of Hydrogen-Bonding to Lipid Lipid Interactions in Membranes and the Role of Lipid Order - Effects of Cholesterol, Increased Phospholipid Unsaturation, and Ethanol. *Biochemistry* 32:3714-3721.

11. Smaby, J. M. and H. L. Brockman. 1990. Surface dipole moments of lipids at the argon-water interface. Similarities among glycerol-ester-based lipids. *Biophys J* 58:195-204.

12. Tocanne, J. F. and J. Teissie. 1990. Ionization of Phospholipids and Phospholipid-Supported Interfacial Lateral Diffusion of Protons in Membrane Model Systems. *Biochimica et Biophysica Acta* 1031:111-142.